UNIVERSITY OF PARDUBICE
FACULTY OF TRANSPORT ENGINEERING

ANTI-SLIP CONTROL OF TRACTION MOTOR OF RAIL VEHICLES

Doctoral Thesis
(Annotation)

2019 Ing. Abdulkadir Zirek

Doctoral: Ing. Abdulkadir Zirek

Programme of Study:

P3710 Technique and Technology in Transport and Communications

Branch of study:

3706V005 Transport Means and Infrastructure

Dissertation Title:

Anti-slip Control of Traction Motor of Rail Vehicles

Author:

Ing. Abdulkadir ZIREK

Supervisor:

Doc. Ing. Michael Lata, Ph.D.

Specialist supervisor:

Prof. Ing. Jaroslav Novák, CSc.

The dissertation has arisen at the supervising:

Department of Transport Means and Infrastructure

ABSTRACT

This work deals with the use of anti-slip control methods for rail vehicles. Initially, to give readers a general picture of the research covered in the thesis, the adhesion and slip mechanism are explained. Furthermore, the slip detection methods and slip control methods based on the literature review are introduced. To verify the validity of the anti-slip control schemes, a numerical model of a tram wheel roller rig that includes nonlinear effects caused by time delay and disturbances to match the values of the experimental test setup has been generated using MATLAB editor. Five wheel slip control strategies -wheel slip control based on single threshold (WSCST), wheel slip control based on multiple thresholds (WSCMT), wheel slip control based on angular acceleration of wheel (WSCAA), PI wheel slip control (PI-WSC), and sliding mode wheel slip control (SM-WSC)- are suggested. In addition to the simulation calculations, this work includes an experimental part in which extensive experiments are carried out on laboratory test equipment where the anti-slip algorithms are implemented and tested. The validity of the developed numerical model is proven with the comparison of the simulation and experimental results. The performances of all the wheel slip control methods are evaluated by the mathematical model and experimental setup. The influences of different roller speeds and control parameters are analysed via validated numeric model.

KEYWORDS

adhesion, wheel slip, anti-slip, acceleration, roller rig, control, PMSM, sliding mode.

NÁZEV

Protiskluzová regulace trakčního motoru železničního vozidla

SOUHRN

Tato práce se proto zabývá využitím metod protiskluzového řízení pohonu kolejových vozidel. Nejprve jsou vysvětleny mechanismy adheze a skluzu. Dále jsou uvedeny metody detekce skluzu a metody regulace. Pro ověření platnosti schémat protiskluzové regulace byl pomocí editoru MATLAB vytvořen numerický model zkušebního laboratorního zařízení tramvajového kola, který obsahuje také nelinearity. Uvedený model se skládá ze synchronního motoru s permanentními magnety, asynchronního motoru, tramvajového kola, kladky (rotující kolejnice) a dvou hnacích hřídelí. Jednu z nelinearit tvoří model mechanismu adheze. Zde je použit model Freibauera a Polacha. Pro detekci a řízení skluzu je použito pět strategií (algoritmů): řízení skluzu kol na základě jednoduché prahové hodnoty (WSCST), řízení skluzu kol na základě více prahových hodnot (WSCMT), řízení skluzu kol na základě úhlového zrychlení kola (WSCAA), PI regulace skluzu kol (PI-WSC) a metoda Sliding Mode Control (SM-WSC). Kromě simulačních výpočtů obsahuje tato práce experimentální část, ve které jsou provedeny rozsáhlé experimenty na zkušebním laboratorním zařízení, kde byly uvedené protiskluzové algoritmy implementovány a testovány. Platnost vyvinutého numerického modelu je prokázána porovnáním simulačních a experimentálních výsledků. Vyhodnoceny jsou vlivy různých parametrů a chování systému při těchto protiskluzových metodách.

KLÍČOVÁ SLOVA

adheze, prokluz kola, protiskluz, zrychlení, zkušební zařízení tramvajového kola a rotující kolejnice, řízení, PMSM

TABLE OF CONTENT

ABSTRACT 2
TABLE OF CONTENT 4
1 INTRODUCTION 6
1.1 Purpose of the Thesis 6
2 THEORETICAL BACKGROUND 7
2.1 Adhesion Phenomenon 7
2.2 Slip Phenomena 8
2.2.1 Problem Formulation 8
2.3 Wheel Slip Identification Methods 9
2.4 Wheel Slip Control Methods 9
3 METHODS AND METHODOLOGY 10
3.1 Experimental Setup 11
3.2 The Numerical Model of Tram Wheel Roller Rig 12
4 DEVELOPED WHEEL SLIP CONTROL METHODS 12
4.1 Wheel Slip Control Based on a Single Threshold 12
4.2 Wheel Slip Control Based on Multiple Thresholds 13
4.3 Wheel Slip Control Based on Angular Acceleration of Wheel 14
4.4 PI Wheel Slip Control 15
4.5 Sliding Mode Wheel Slip Control 16
5 RESULTS AND DISCUSSION 18
5.1 Validation of Numerical Model 18
5.2 Simulation Results 19
5.2.1 Wheel Slip Control Based on a Single Threshold 19
5.2.2 Wheel Slip Control Based on Multiple Thresholds 20
5.2.3 Wheel Slip Control Based on Angular Acceleration of Wheel 21
5.2.4 PI Wheel Slip Control 22
5.2.5 Sliding Mode Wheel Slip Control 23
5.3 Experimental Results 24

5.3.1 Wheel Slip Control Based on a Single Threshold 24
5.3.2 Wheel Slip Control Based on Multiple Thresholds 25
5.3.3 Wheel Slip Control Based on Angular Acceleration of Wheel 26
5.3.4 PI Wheel Slip Control 27
5.3.5 Sliding Mode Wheel Slip Control 28
5.4 Analysis of Results 29
6 CONCLUSION 31
6.1 Completed Objectives of Doctoral Thesis 32
6.2 Scientific Contributions of Doctoral Thesis 32
6.3 Future Works 33
REFERENCES 34
PUBLICATIONS OF STUDENT 37

1 INTRODUCTION

Due to the demand and emerging technologies in the railway sector, more powerful rail vehicles have been recently produced. The current development in the power capacity of the vehicles drive systems enables them reaching high torques in a short time. The tractive effort of vehicle is transferred to the rail in a small contact area that provides the vehicle with an advantage due to the lower power losses caused by friction in wheel-rail contact [1]. On the other hand, the traction ability of these vehicles is limited to environmental conditions (i.e. rain, snow, leaves and mud) and human influences. Besides, the adhesion between wheel and rail decreases with the increase of the running speed under contaminated surface conditions [2]. All these factors lead the slip of the wheel, which occurs when tractive effort exceeds the available adhesion, whereas sliding occurs when the braking effort exceeds the available adhesion. If the slip/slide reaches the high value, it causes severe wear of wheel and rail surfaces, increasing mechanical stress in the system and affects stability. The presence of high wheel slip is an undesired situation resulting in a reduction in the safety, traction performance and wheel-rail lifetime.

Due to requirements anti-slip, control systems have been developed. In the early age of railway transportation, the vehicles were equipped with the sander which improves the adhesion conditions. However, the sanding increases 10 to 100 times the wheel and rail wear [1], [3]. Thus, new strategies were sought out to be used for rail vehicles. In the late 70s, thanks to the rapid development of automatic control strategies and electronic technologies, the microprocessors with online processing were used for the detection of wheel slip and torque adjustment [4]. The first developed wheel slip control methods are the re-adhesion controller. The conventional re-adhesion control methods use the wheel slip speed or acceleration criterions to detect wheel slip. The methods do not require exact information of the wheel-rail contact condition for wheel slip detection and compensation of poor adhesion [4]. However, such strategies do not stop the wheel slip formation but suppress it. Due to the requirements of the trains hauled by locomotives, more advanced wheel slip control strategies are developed. The methods aim to stabilise the wheel slip at the peak of the slip curve to establish the optimum utilisation of the adhesion characteristic. Although there is a vast amount of literature on both re-adhesion and wheel slip control strategies, there is still a need for further investigations.

1.1 Purpose of the Thesis

The basic premises of this study are summarised as follows:

(i) Summarising a large number of published studies on the wheel slip, adhesion and slip control methods.

(ii) Reproducing a numerical model of the tram wheel roller rig in MATLAB environment that can be used for performance evaluation of the wheel slip control strategies.

(iii) Proposing algorithms to control the wheel slip mechanism and establishing optimum utilisation of adhesion.

(iv) Validation of reproduced numeric model.

(v) Verifying the functionality of proposed wheel slip control algorithms by either the validated numerical model or experimentally obtained results from the tram wheel roller rig.

(vi) Performance evaluation of the proposed wheel slip control algorithms with different speeds and control parameters.

2 THEORETICAL BACKGROUND

2.1 Adhesion Phenomenon

The coefficient of the adhesion is usually represented by the ratio of the traction force (T) and the normal force (N). The free body diagram of a driven wheel is presented in Figure 1, while the coefficient of the adhesion can be calculated using Eq. 1.

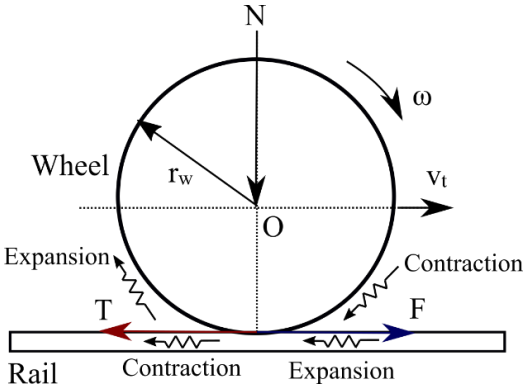

Figure 1. The forces and velocities acting on a driven wheel.

$$\mu = \frac{T}{N} \qquad \textit{Eq. 1}$$

where T is traction force, N is normal load force, and μ is the coefficient of adhesion.

The loss of adhesion between wheel and rail can adversely influence the traction and braking effort of the vehicles. As it is mentioned below, poor adhesion causes wheel slip during the traction process and leads to the damage of wheel and rail [5]. Recently, various approaches have been proposed to outline

the reasons for the loss of the adhesion [2], [6]–[9]. Overall, these studies show that the loss of adhesion may occur due to the presence of water (rain, snow, dew), oil, and leaf contaminants. Moreover, the temperature is another factor which influences the adhesion.

2.2 Slip Phenomena

The most common definition of the wheel slip in the railway area is the normalised difference of the angular and longitudinal velocities of the vehicle. The wheel slip occurs when the tractive effort of the vehicle exceeds the adhesion force, whereas sliding occurs when the braking force exceeds the adhesion force.

The adhesion is defined as a function of the slip at the contact point of the wheel and rail [10]. The slip velocity and relative slip (hereinafter is referred to as wheel slip) can be calculated using the Eq. 2 and Eq. 3 as given below.

$$w_s = \omega \cdot r_w - v_t \qquad \textit{Eq. 2}$$

$$s = \frac{\omega \cdot r_w - v_t}{v_t} \qquad \textit{Eq. 3}$$

where w_s is slip speed, v_t is the vehicle longitudinal speed, ω is the wheel rotational speed, r_w is wheel radius, and s is the wheel slip.

2.2.1 Problem Formulation

A certain amount of wheel slip is required to transfer the tractive effort from the wheel to the rail. As it is illustrated in Figure 2, the slip curve has a nonlinear characteristic. The area on the left side of the peak of the slip curve is called adhesion zone while the one on the right side of the peak is the slip zone. The adhesion zone is stable, and adhesion proportionally increases with the wheel slip. On the other hand, the slip zone is nonstable part of the curve, and adhesion decreases when the wheel slip increases. Most of the wheel slip control methods aim to keep the slip in the stable part of the curve. While the main goals of the optimisation methods are to control the slip toward the peak of the curve where the maximum traction effort is achieved at [11]. Therefore, in this study, conventional and novel wheel slip control strategies are implemented to control the wheel slip toward the peak of the slip curve. The operation zone of the controllers is limited with the stable and the unstable parts of the slip curve near the maximum point [1].

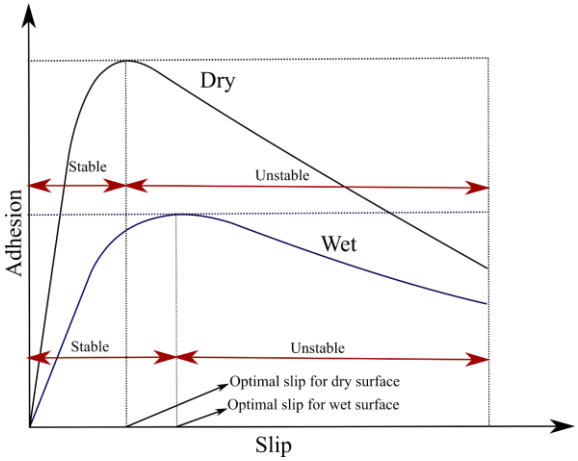

Figure 2. Slip-adhesion curve illustrating the characteristic of CoA under dry and wet contact conditions.

2.3 Wheel Slip Identification Methods

The most common wheel slip identification methods are summarised as follows:

- Current-based wheel slip detection of the all-wheel driving vehicle [12]
- Using the speed difference of driven and non-driven wheels [13].
- Method based time-frequency analysis [14]
- Linear, nonlinear and Kalman filters [15], [16].
- Nonlinear observers [17], [18].
- Using global positioning Systems (GPS) [19].
- Use of the optical-based sensor [20].

2.4 Wheel Slip Control Methods

Recently, various wheel slip control methods have been put forward to solve the issue of high slip between the wheel and rail. Pichlík [13] classified the wheel slip control method in two categories which are used for the electric multiple units (EMU) and the locomotives. According to Pichlík, the wheel slip control methods that are used in EMU aim to prevent the high value of slip velocity; thus, these methods reduce the power loses and wear of the vehicle wheels and rails. The wheel slip control methods for locomotive aim to achieve maximum adhesion rather than preventing the wheel slip [13]. Kondo explains the reason for this classification due to axle loads of the EMU and locomotive [21]. Since the axle loads of the EMU is lower than the locomotive, the adhesive region is too narrow to control the adhesion at the peak of the slip curve precisely. The wheel slip control methods for EMU and locomotives are the main interest of

this work. Therefore, the current work deals with wheel slip control algorithms in general. Frylmark and Johnsson have summarised the most common wheel slip control methods, as indicated in Figure 3 [11]:

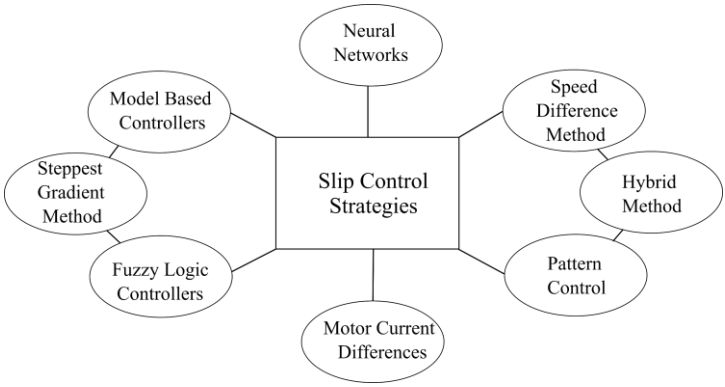

Figure 3. The wheel slip control strategies [11].

Besides the strategies mentioned above, angular acceleration-based control methods and PID (proportional, integral and derivative) control methods are some of the other control strategies used for the slip control. The basic principles of the mentioned methods are described in the following sections. The further details are available in the thesis.

3 METHODS AND METHODOLOGY

Performing on-track tests of railway vehicles are challenging, time-consuming and less cost effective. In keeping with the purpose of the study, the whole vehicle can be reduced to one powered bogie or a single wheelset [22]. Since the dynamics of the drive system are the main interest, a full-scale tram wheel roller rig is used for validation of the control algorithms. For experimental tests, the vehicle is replaced by a tram wheel that is connected to a permanent magnet synchronous motor with the rail being replaced by a roller connected to an asynchronous motor. These substitutions differ from the actual case. More detailed information about the replacements and their effects are presented by Voltr [23] and Gerlici et al. [24].

In this thesis, the performances of the wheel slip control algorithms are investigated using a full-scale tram wheel roller rig and its numerical model that is generated in MATLAB editor.

3.1 Experimental Setup

The experiments are performed on the tram wheel roller rig, which was constructed by VÚKV (Výzkum, Vývoj a Zkušebnictví Kolejových Vozidel) and was renewed by the Faculty of Transport Engineering for further research. The tram wheel roller rig is composed of three main parts; a tram wheel, a roller, and a mainframe. The roller, which is manufactured from a railway wagon wheel, represents the rotating rail [25]. The roller is connected to the AM, which keeps the system at a constant speed by providing opposing torque. A schematic view and photos of the full-scale tram wheel roller rig are presented in Figure 4 and Figure 5, respectively. The details about the experimental test stand are provided in the thesis.

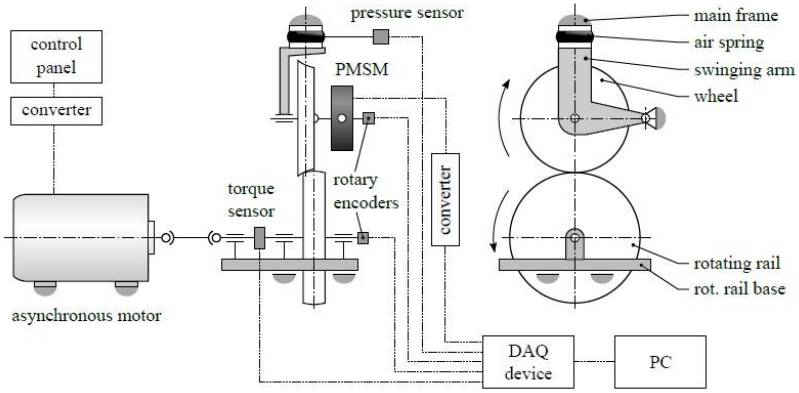

Figure 4. Schematic view of full-scale tram wheel roller rig measurement configuration [26].

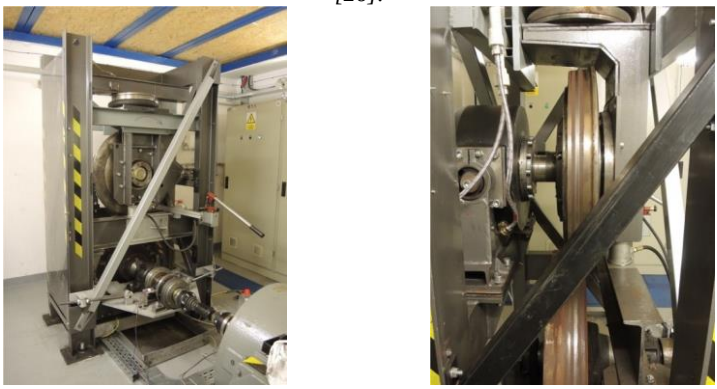

Figure 5. The full-scale tram wheel roller rig [22],[27].

3.2 The Numerical Model of Tram Wheel Roller Rig

In order to evaluate the performance of the developed wheel slip control methods, a numerical model representing the tram wheel roller rig has been generated in the MATLAB environment. The numerical model consists of five main components: the mechanical model of the torsional system, the dynamic model of the PMSM, dynamic model of the AM, the Freibauer/Polach adhesion force model, and the anti-slip control model. All the components of the numerical model are explained in detail in the thesis. The finite difference method is used for the calculation of the dynamic equations. The step time of integration is selected as $20\ \mu s$ to guarantee the accuracy of the calculations. However, the control action of the anti-slip control model is limited to the period of $0.04\ ms$ to simulate the control action of the controller in the real tram wheel roller rig. The complete structure of the developed numerical model tram wheel roller rig is depicted in Figure 6.

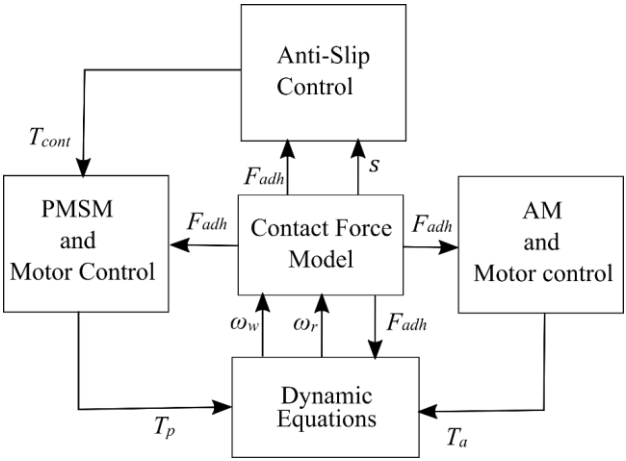

Figure 6. Complete structure of developed numerical model of tram wheel roller rig.

4 DEVELOPED WHEEL SLIP CONTROL METHODS

4.1 Wheel Slip Control Based on a Single Threshold

The wheel slip control based on a single threshold (WSCST) is a conventional method. The principle of the method is illustrated graphically in Figure 7. The actual value of wheel slip is compared with a constant threshold value. If actual wheel slip exceeds the threshold value, the controller regulates the applied torque according to Eq. 4. The block diagram of the controller is depicted in Figure 8. The output of the torque regulator is limited to prevent excessive torque increase. The output torque request of the limiter is compared

with the driver torque request. The smaller torque request is selected as control torque.

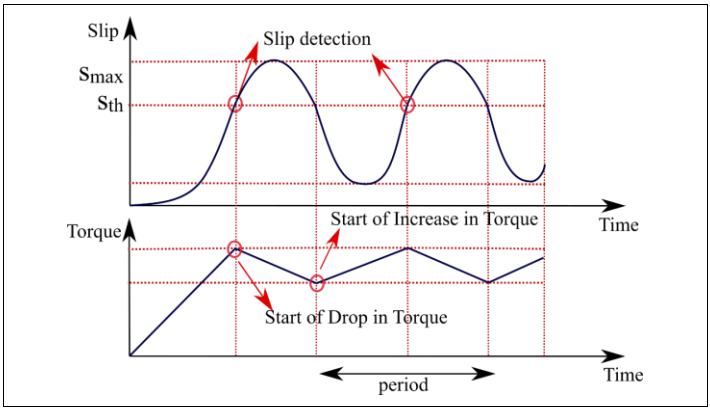

Figure 7. Wheel slip detection and torque regulation for WSCST.

$$T_{ref}^{*} = \begin{cases} T_{cont}\,(1 - \dfrac{dt}{A_{dec}}), & s_{act} \geq s_{th} \\ T_{cont}\,(1 + \dfrac{dt}{A_{inc}}), & s_{act} < s_{th} \end{cases} \qquad \textit{Eq. 4}$$

where T_{ref}^{*} is the reference torque output of the controller, T_{cont} is the final output torque request, dt is the resolution time of speed sensor, A_{dec} is the control parameter which determines the deceleration rate of torque, A_{inc} is the control parameter which determines the increment rate of the torque, s_{th} is the slip threshold value, and s_{act} is the actual wheel slip occurs between the wheel and the roller.

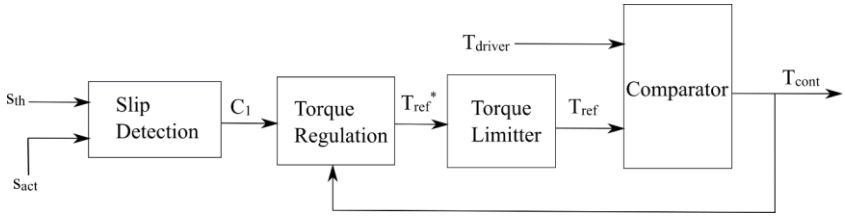

Figure 8. Block diagram of WSCST.

4.2 Wheel Slip Control Based on Multiple Thresholds

Wheel slip control based on multiple thresholds (WSCMT) is an improved version of the abovementioned method (WSCST). To prevent extreme torque drop and increase, two threshold values are employed. Both threshold values are assigned in the stable part of the slip curve. The control action of the developed

control is illustrated graphically in Figure 9. The torque regulation of the motor is provided by Eq. 5. The WSCMT is expected to provide less wheel slip and better adhesion utilisation than the WSCST.

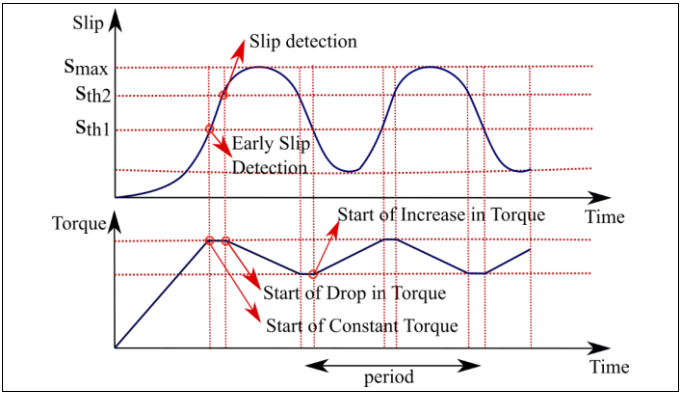

Figure 9. Wheel slip detection and torque regulation with multiple threshold values.

$$T_{ref}^{*} = \begin{cases} T_{cont}\,(1 - \dfrac{dt}{A_{dec}}), & s_{act} \geq s_{th2} \\ T_{cont}\,, & s_{th1} \leq s_{act} \leq s_{th2} \\ T_{cont}\,(1 + \dfrac{dt}{A_{inc}}), & s_{act} < s_{th1} \end{cases} \qquad \textit{Eq. 5}$$

where s_{th1} is the first threshold value, and s_{th2} is the second threshold value.

4.3 Wheel Slip Control Based on Angular Acceleration of Wheel

The wheel slip control based on the angular acceleration of wheel (WSCAA) is a conventional method. It is based on the principle that the angular acceleration of a vehicle wheel, provided that it rolls without slip, is equal to linear acceleration of the vehicle divided by the wheel radius. The acceleration of the vehicle is limited by the inertia of the vehicle and the traction force. If the wheel shows higher angular acceleration than what corresponds to this limit, it means that it accelerates independently of the vehicle motion – in other words, it slips.

The control action WSCAA is summarised in Figure 10. The wheel slip is detected through comparison of actual angular acceleration and the threshold value of the acceleration. When the actual value of acceleration exceeds the threshold value, the controller reduces toque request according to Eq. 6 until it becomes lower than the threshold. Then, the torque request rises again. The action of the controller takes place periodically until the bad contact conditions disappear.

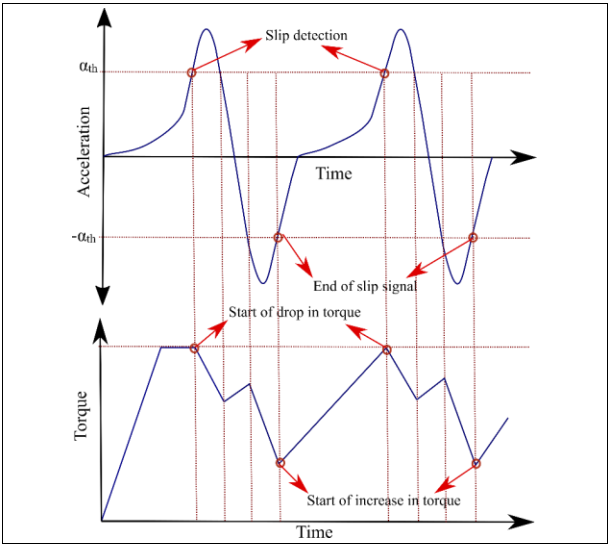

Figure 10. Wheel slip detection and torque regulation of WSCAA.

$$T^*_{ref} = \begin{cases} T_{cont}\,(1 - \dfrac{dt}{A_{dec}}), & \alpha_{act} \geq \alpha_{th} \;||\; \alpha_{act} \leq -\alpha_{th} \\ T_{cont}\,(1 + \dfrac{dt}{A_{inc}}), & \alpha_{act} < \alpha_{th} || \; \alpha_{act} \geq -\alpha_{th} \end{cases} \qquad \textit{Eq. 6}$$

where α_{act} is the actual angular acceleration of the wheel and α_{th} is the threshold value of angular acceleration for the wheel slip detection

4.4 PI Wheel Slip Control

The PI control strategy is widely used for industrial applications. The PI controller can be used for the rail vehicles to control wheel slip and improve their traction performance. For effective control, a reference slip value that is close to the peak of the slip curve can be chosen as a control signal. It is also essential that the selected reference wheel slip value is on the stable side of the slip curve.

The discrete time form of a PI controller is expressed as in Eq. 7.

$$u(k) = u(k-1) + K_p\big(e(k) - e(k-1)\big) + K_i e(k) \qquad \textit{Eq. 7}$$

where u is the output torque of the controller, K_p is the proportional gain of the controller, K_i is the integral gain of the controller, k is the iterative step, e is the error between the actual wheel slip and desired wheel slip. The error is calculated, as shown in Eq. 8.

$$e(k) = s_d - s_{act}(k) \qquad \textit{Eq. 8}$$

where s_d is the desired wheel slip value, and s_{act} is the actual wheel slip value.

The block diagram of the PI wheel slip control method (PI-WSC) is provided in Figure 11. The difference between the desired wheel slip and actual wheel slip (error) is calculated first and then sent to the PI torque regulator as an input signal. The PI torque controller regulates the torque applied to wheel according to the error signal.

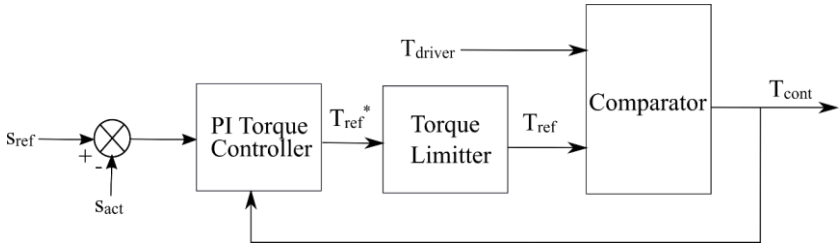

Figure 11. Block diagram for PI-WSC.

4.5 Sliding Mode Wheel Slip Control

The sliding mode controller (SMC) has been widely-studied for vehicle control systems because of certain advantages [33]–[35]. The controller is an attractive robust control method with effective properties to stabilise nonlinear and uncertain systems. The controller keeps the systems insensitive to uncertainties on a sliding surface. Moreover, the SMC has good and rapid transient performance [36].

The sliding mode wheel slip controller (SM-WSC) is designed in two steps. In the first step, the sliding surface is defined to obtain specific desired characteristics along the sliding surface trajectories. Next, the controller is designed to lead the system to the desired system trajectories within a finite time.

The sliding surface *S(t)* for the design of the adaptive sliding mode torque control systems is defined as follows:

$$S(t) = s - s_d \qquad \textit{Eq. 9}$$

The main objective of Eq. 9 is to track the desired wheel slip ratio (s_d) that is given as an input to the system, based on experience from previous experimental measurements. In order to satisfy the reachability conditions directing the system trajectories toward a sliding surface where they remain, the derivative of the sliding surface is selected as Eq. 10 [37], [38]:

$$\dot{S} = -DS - K \cdot sgn(S) = -D(s - s_d) - K \cdot sgn(s - s_d) \cdot \qquad \textit{Eq. 10}$$

where the proportional term-*DS* forces the system state to approach the sliding surface faster when the sliding surface has a significant value [33]. The parameters *D* and *K* are positive definite design parameters. *D* determines the

convergence rate of the tracking error, while *K* is adjusted in compliance with the number of uncertainties and the disturbance in the system.

The *sgn* function in Eq. 10 results in a chattering issue because of undesired noise and delays in the actuator. For this reason, the *sgn* function is replaced with a saturation function [39]. Nevertheless, a lowpass filter is implemented to overcome the high-frequency chattering problem in the system, which is basically to stabilise the algorithm.

The sliding mode control law is designed in the following steps, according to Eq. 10.

The wheel slip dynamics during acceleration obtained by taking the time derivative of Eq. 3.

$$\dot{s} = r_w \frac{\dot{\omega_w}}{r_r\,|\omega_r\,|} - r_w \frac{\omega_w\,|\dot{\omega_r}\,|}{r_r\,\omega_r^2} \qquad \textit{Eq. 11}$$

The relationship between the wheel slip dynamic and forces at the contact point is shown in Eq. 11.

$$\dot{s} = r_w \frac{-T_w - r_w\,F_{adh}}{J_w\,r_r\,|\omega_r\,|} - r_w \frac{\omega_w\,|\dot{\omega_r}\,|}{r_r\,\omega_r^2} + d \qquad \textit{Eq. 12}$$

where *d* is disturbance due to vibration in the system, driving resistances and parameter uncertainties.

By taking the time difference of the sliding surface in Eq. 9, and substituting Eq. 10 and Eq. 12, the following sliding law control torque can be achieved:

$$T_{p,con} = -r_w\,F_{adh} - \frac{J_w\,\omega_w\,|\dot{\omega_r}|}{|\omega_r\,|} - \frac{J_w\,r_r\,|\omega_r\,|(-D(s-s_d\,) - K\cdot sgn(s-s_d\,))}{r_w} - \frac{J_w\,r_r\,|\omega_r\,|\dot{s_d}}{r_w} \qquad \textit{Eq. 13}$$

Since the time derivative of s_d constant is zero and the acceleration value of the roller is neglected for the tram wheel roller rig, the sliding mode control law torque is modified to the following equation:

$$T_{p,con} = -r_w\,F_{adh} - \frac{J_w\,r_r\,|\omega_r\,|D(s-s_d\,)}{r_w} - \frac{J_w\,r_r\,|\omega_r\,|K\cdot sgn(s-s_d\,)}{r_w} \qquad \textit{Eq. 14}$$

Asymptotical stability of the sliding mode control law can be proven for closed-loop control by employing a Lyapunov function [33], [39].

5 RESULTS AND DISCUSSION

5.1 Validation of Numerical Model

In order to use the developed numerical model of the tram wheel roller rig for the performance evaluation of the implemented wheel slip control strategies, the validity of the model has to be proven. Hence, the numerical model is tested without any wheel slip controller. Figure 12 shows the comparison of the simulation and experimental results carried out under water contaminated conditions. The tests are performed for the same PMSM torque request (Figure 12(a)). The resultant wheel slips are in good agreement which can be seen in Figure 12(b). Besides, the slip curves of simulation and experiment are presented in Figure 12(c). The slender clockwise loops observed in experiment results are closely simulated by the numeric model. Furthermore, slight differences between the simulation and experimental wheel speed results are displayed in Figure 12(d).

Even though the simulated performance characterised the experimental response satisfactorily, differences established between experimental and numerical results (Figure 12). The pre-assumed simplifications in the model which does not include all mechanical details and imperfections of the real experimental device and testing conditions yield the first group of factors causing mentioned differences. Other factors are related to the measurement procedure including parasitic signals (mainly electromagnetic noise), resolution of sensors, as well as processing the simulation results – filtering which impacts the signals particularly when wheel slip is suddenly terminated.

Despite the effects of mentioned factors, it is seen that the results obtained from the developed numerical model are consistent with the experimental results. This fact proves the validity of the developed numerical model.

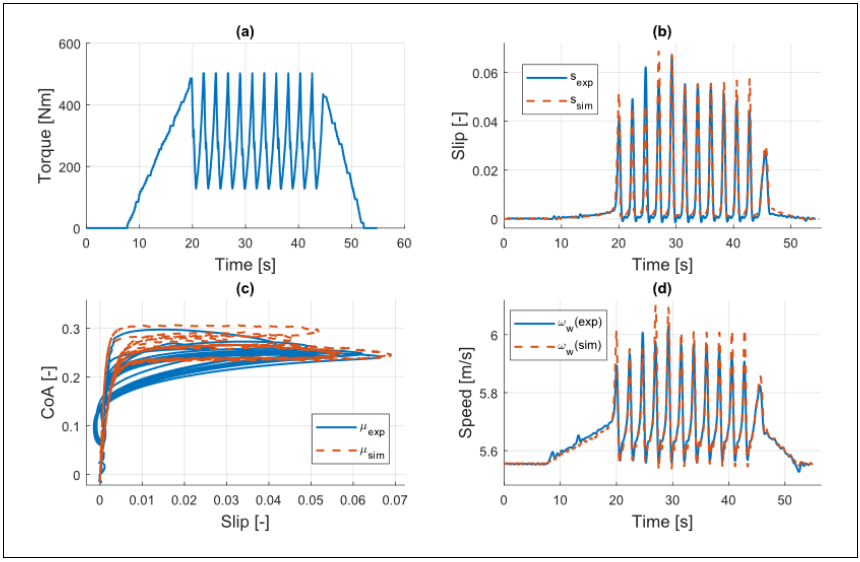

Figure 12. The comparison of the simulation and experimental results.

5.2 Simulation Results

The step time of the integrations is selected as *20 μs* to guarantee the accuracy of calculations. However, the control action of the anti-slip control models is limited to the period of *0.04 ms* to simulate the control action of the controller in the real tram wheel roller rig. The initial peripheral speed of the roller is selected as *5.56 m/s*, which corresponds to *20 km/h* for a tram vehicle, in the simulations. To be able to observe wheel slip in low torque value, the normal force is assigned relatively small. Hence, the normal force is provided to the simulation as an average value of *4250 N*.

5.2.1 Wheel Slip Control Based on a Single Threshold

The initial test for WSCST is carried out under the assumption of continuous water contaminated test conditions. The control parameters are selected as; $s_{th}=0.01$, $A_{inc}=1$ and $A_{dec}=0.5$. The minimum torque (T_{min}) generated by the WSCST controller is set as *15%* of the nominal torque of PMSM. It is assumed that the water is continuously supplied to the contact area. The simulation results are illustrated in Figure 13. It can be seen in Figure 13(c), wheel slip is controlled cyclically. However, the amplitude and the frequency of the cycles are not constant due to the nonlinearity, and numerical errors. The response of the controller is sufficient since the maximum wheel slip ever to occur is merely *7.4%*.

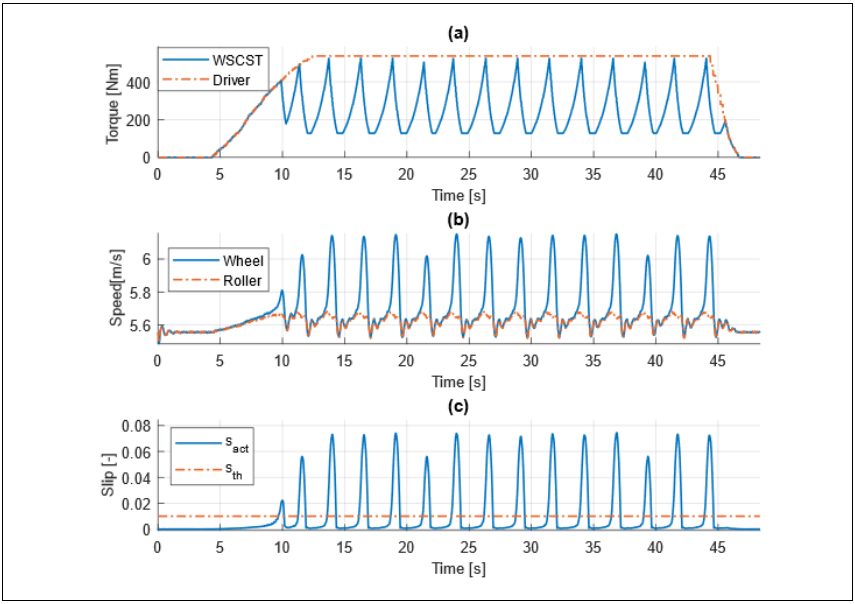

Figure 13. Simulation result of WSCST performed under the assumption of water contaminated test condition.

The second simulation is carried out to investigate the performance of WSCST under the assumption of steady grease contaminated test condition. The control parameters are set as; $s_{th}=0.015$, $A_{inc}=2$ and $A_{dec}=1$. T_{min} is selected 1% of the nominal torque of PMSM. The results are presented in Figure 29 of the thesis. Similar to the previous simulation, the wheel slip is controlled cyclically. The dynamic behaviour (non-periodic response, irregular cycles, i.e.) of the wheel slip observed are caused by the uncertainties and numerical errors. The WSCST achieves a successful control within *4.1%* maximum wheel slip.

5.2.2 Wheel Slip Control Based on Multiple Thresholds

The performance of the controller is initially tested under the assumption of the continuous water existing between the wheel and roller. The control parameters are set as; $s_{th2}=0.006$, $s_{th1}=0.008$, $A_{inc}=4$ and $A_{dec}=1$. The minimum torque (T_{min}) generated by the WSCMT is set as *15%* of the nominal torque of PMSM. When Figure 14(c) is analysed, it can be seen that the maximum wheel slip of *2.3%* is observed during the simulation. Moreover, it is found in Figure 14 (a) that the minimum torque the output of WSCMT is *224 N.m*. Overall, the controller provides an improvement in the traction characteristic of the wheel.

The performance of the controller is tested under the assumption of steady grease contaminant existing between the wheel and the roller. The results are

presented in Figure 31 of the thesis. Maximum wheel slip of *4%* occurs. When the output of the controller is examined, it is noticed that the minimum torque is *62 N.m*. From the results, it is possible to claim that the controller prevents the wheel from the severe slip effectively. Furthermore, the controller reduces the amount of torque drop slightly.

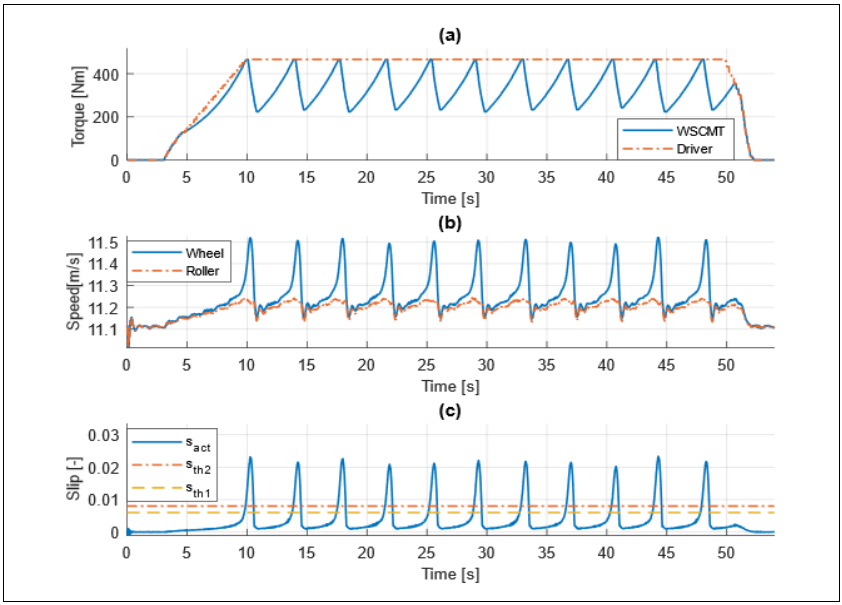

Figure 14. Simulation result of WSCMT performed under the assumption of water contaminated test condition.

5.2.3 Wheel Slip Control Based on Angular Acceleration of Wheel

To confirm the operation verification of the WSCAA method, we conduct the first simulation under the assumption of water contaminated test condition. The control parameters are selected as; $\alpha_{th}=1$, $A_{inc}=1$ and $A_{dec}=0.5$. The simulation is conducted for two different cases of wheel-roller surface conditions which are half-dry and wet. The resultant wheel slip is depicted in Figure 15(b). During the first cycle, the wheel slip raises to *8.6%* on the other hand, in the next cycles, the peaks of the wheel slip are noticed around *5.9%*. The results have proved that WSCAA can avoid severe wheel slip when the sudden changes occur in adhesion condition.

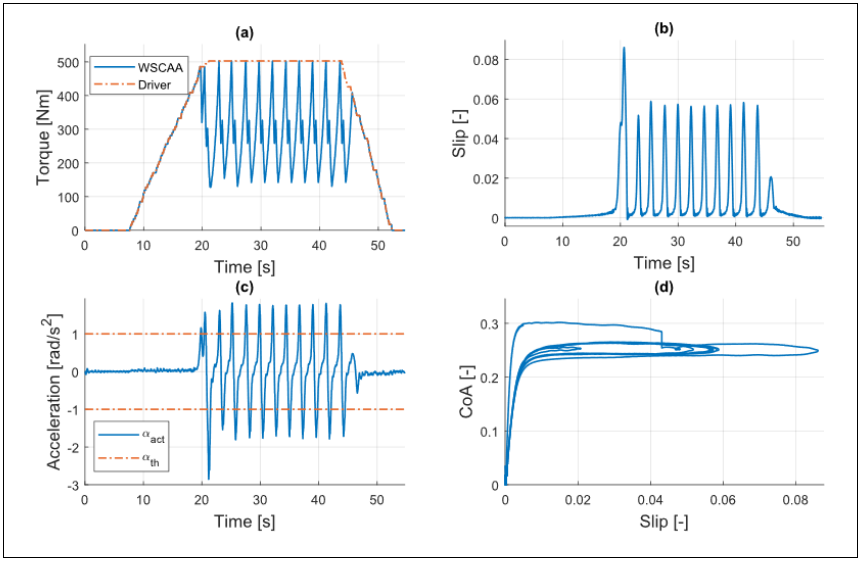

Figure 15. Simulation result of WSCAA performed under the assumption of water contaminated test condition.

Another simulation is carried out under the assumption of grease contaminated test condition. The results are depicted in Figure 33 of the thesis. It is noticed that during the first cycle; the wheel slip raises to *9.9%*. In the next cycles, the peaks are observed at *7%*. It is seen that the WSCAA provides a successful wheel slip control during the low adhesion condition.

5.2.4 PI Wheel Slip Control

The initial test is conducted under the assumption of the continuous water contaminant existing between the wheel and roller. The control parameters are set as; $s_d=0.01$, $K_p=500$ and $K_i=2000$. The response of the controller is presented in Figure 16. The desired wheel slip ($s_d=0.01$) is reached successfully, as illustrated in Figure 16(b). Moreover, the desired wheel slip corresponds to the peak of the slip curve, as depicted in Figure 16(c). When the path of the wheel slip is analysed, no significant overshoot is observed.

The second simulation is carried out to test the reaction of the PI-WSC method toward the sudden change of the friction condition. The presented results (see Figure 35 for further information in the thesis) show that the controller stabilises the wheel slip at *1%* in a short time. Because of the sudden change of the friction condition, the wheel slip increases up to *11.5%*.

The last simulation is conducted with the assumption of the steady grease contaminated test conditions. It is observed that the controller effectively

stabilises the wheel slip at the desired level with a slight overshoot. Furthermore, the desired level corresponds to the peak of the slip curve. The results are presented in Figure 36 of the thesis.

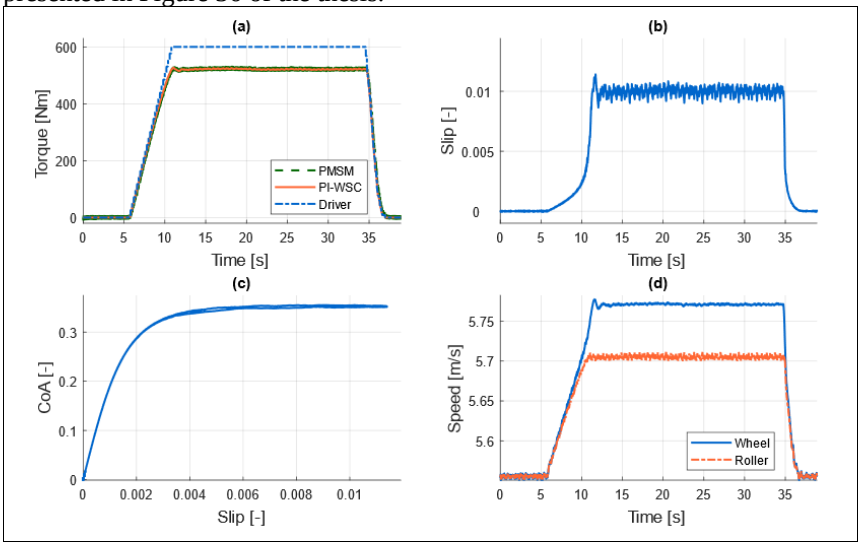

Figure 16. Simulation results of PI-WSC performed under the assumption of water contaminated test condition.

5.2.5 Sliding Mode Wheel Slip Control

To verify the effectiveness of the developed control method, we performed the initial tests using the validated numeric model. The following values are selected for the control parameters; *D=10, K=1 and* s_d*=0.02.*

The simulation results of SM-WSC performed under the assumption of water contaminated test condition can be seen in Figure 17. Two phases of the adhesion scenario are selected for the simulation of water contamination (Half-dry and wet). The controller effectively stabilises the wheel slip at *2%*, as seen in Figure 17(b). The maximum overshoot displayed in the wheel slip is about *5.1%*, which has a relatively low value. Moreover, the indicated results demonstrate the effective performance of the proposed strategy since the wheel slip is stabilised almost at the peak of the slip curve (see Figure 17c).

Similar performances observed for the simulation which is carried out under the assumption of steady grease contaminant. The results are available in Figure 38 of the thesis. The presented results confirm the functionality of the controller.

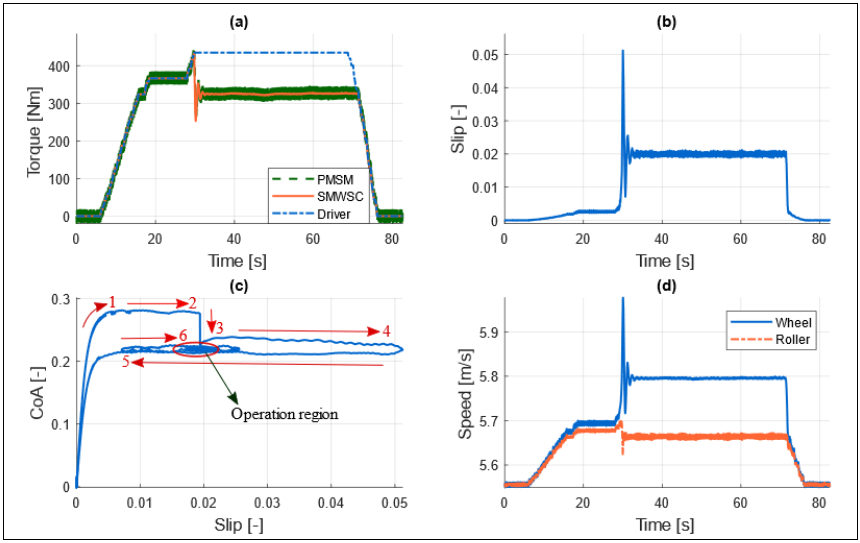

Figure 17. Simulation results of SM-WSC performed under the assumption of water contaminated test condition.

5.3 Experimental Results

The sampling rate of data logger that is connected to the test stand is *200 Hz*. However, the control action of the anti-slip algorithm is limited with *25 Hz* to gain time for data processing. The initial peripheral speed of the roller is selected as *5.56 m/s*, which corresponds to *20 km/h* for a tram vehicle. The air spring provides no air pressure to obtain the higher wheel slip with lower traction torque. On the other hand, the average of the normal force is measured as *4250 N*, due to self-weights of the wheel, air spring and swinging arm.

5.3.1 Wheel Slip Control Based on a Single Threshold

Figure 18 shows the experimental results of WSCST performed under water contaminated test condition. The resultant wheel slip is provided in Figure 18(c). The controller prevents the severe wheel slip effectively where maximum wheel slip of *8.1%* is seen.

The experimental test results of WSCST under the steady grease contaminated test condition are presented in Figure 40 of the thesis. The results are quite similar to findings under the water contaminated condition. The wheel slip is suppressed successfully with a maximum of *4%*.

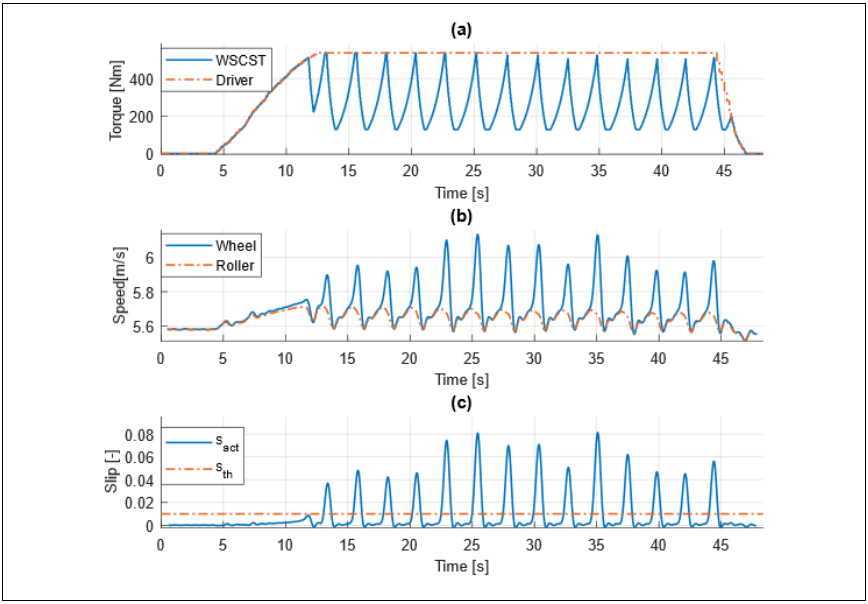

Figure 18. Experimental result of WSCST performed under water contaminated test condition.

5.3.2 Wheel Slip Control Based on Multiple Thresholds

The performance of the WSCMT is verified with the help of the experimental tram wheel roller rig. The initial roller speed is set as *11.2 m/s* that approximately corresponds to *40 km/h* for a tram vehicle.

Figure 19 shows the response of the WSCMT carried out under the continuous water contaminated test condition. The proposed algorithm appears to deliver a satisfactory performance since the strategy provides a cyclic control of wheel slip where the peaks are noticed between *1.3-2%*. Besides, the controller prevents the wheel from the excessive torque drops, which reduce traction performance.

The results of the experiment which are conducted under the steady grease contaminated test condition are provided in Figure 42 of the thesis. When the presented results are analysed, the controller suppresses the severe wheel slip effectively since the peaks of the cycles are found to be around *4.4%*.

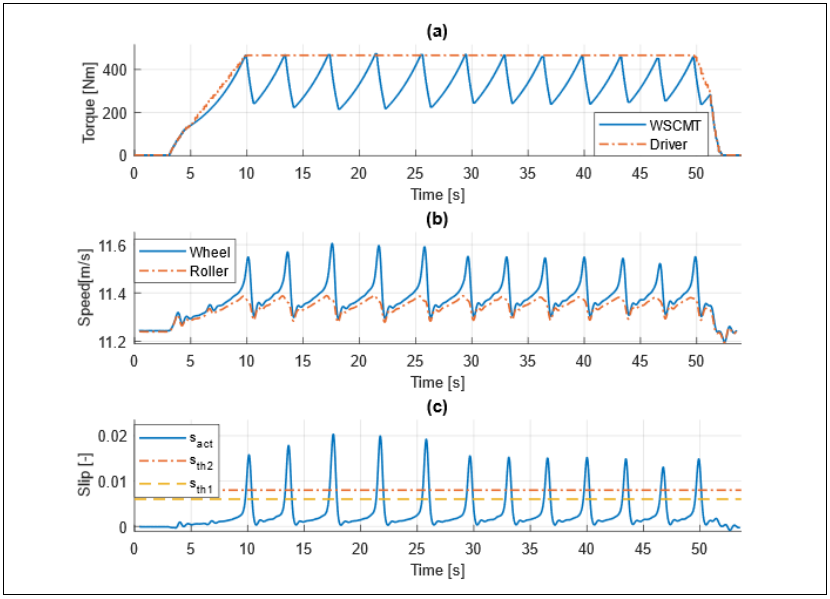

Figure 19. The experiment result of WSCMT performed under water contaminated test condition.

5.3.3 Wheel Slip Control Based on Angular Acceleration of Wheel

To confirm the operation of the WSCAA, we conducted the first experimental test under water contaminated test condition (half-dry and wet). The wheel slip control performance of WSCAA is depicted in Figure 20(b). During the first five cycles of the control process, the magnitude of the peak of the wheel slip tends to increase while the magnitude of the peak of wheel slip reduces gradually in the subsequent cycles. A maximum wheel slip of *6.7%* is observed during the test.

Similar performances are observed for the steady grease contaminated wheel-roller surface conditions which are presented in Figure 46 of the thesis. Due to the system delay, a sudden wheel slip occurs at the first cycle, and then, the controller reduces the wheel slip to lower values in the next cycles. The peaks of the wheel slip cycles are observed around *5.9%*.

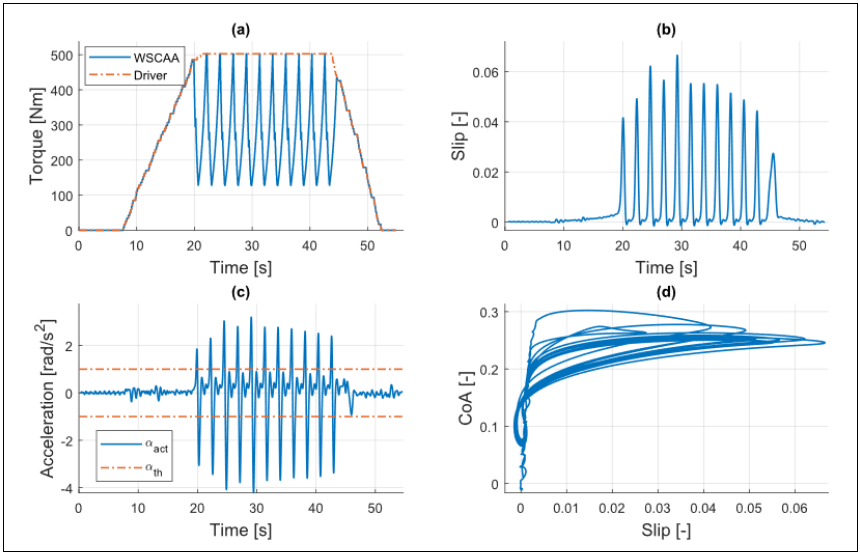

Figure 20. Experimental result of WSCAA performed under water contaminated test condition.

5.3.4 PI Wheel Slip Control

The operation of the PI-WSC is verified initially under the continuous water contaminated test conditions. The controller stabilises the desired wheel slip, as given in Figure 21(b). Closer inspection to Figure 21(c) shows that the controller operates at the peak of the slip curve. Surprisingly, a constant difference between the wheel and roller speeds is observed in Figure 21(d), even at free rolling. This difference causes an offset in the calculated wheel slip value.

Another experimental test is carried out to examine the dynamic response of the controller to the sudden decrease in the friction condition (half-dry to wet). The results are provided in Figure 48 of the thesis. The controller provides a successful control since the recovery from the unstable side of the slip curve to the stable side of the slip curve takes in an instant. The PI-WSC stabilises the wheel slip at *1%* (for both conditions of adhesion) which corresponds to the peak of the slip curve for the water contaminated test condition.

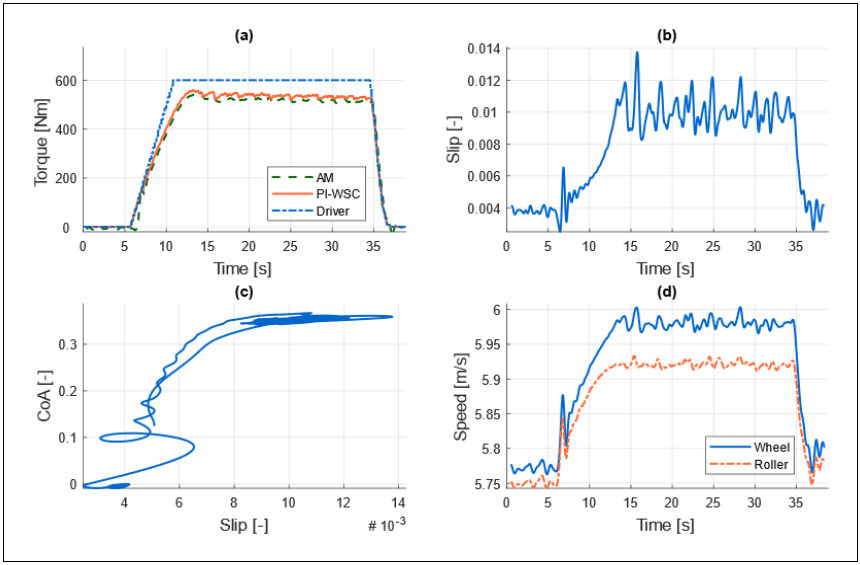

Figure 21. Experimental results of PI-WSC performed under water contaminated test condition.

5.3.5 Sliding Mode Wheel Slip Control

The experimental results of the proposed algorithm performed under water contaminated wheel-roller surface conditions are presented in depth in Figure 22. The resultant wheel slip is provided in Figure 22(b). The SM-WSC is activated right after the wheel slip value reaches beyond the desired amount (*2%*). The controller reduces the motor torque, as indicated in Figure 22(a), and the wheel slip is stabilised at *2%*. A maximum wheel slip of *7%* is observed during this test.

The performance of the controller under the steady grease contaminated test condition is very effective where the wheel slip on *2%* level is successfully established, as indicated in Figure 50 of the thesis. Moreover, it is seen that *2%* of wheel slip corresponds to a point where the maximum adhesion is seen.

One of the interesting results is observed during the test with grease and water&grease contaminated conditions. When the water is sprayed on to the grease contaminated surface, the available adhesion drops severely. Furthermore, the water particles removed from the contact surface when the application of water is stopped. It is seen that the SM-WSC stabilises the wheel slip at *2%* within all case of the adhesion conditions. Here, it must be noted that *2%* of the wheel slip corresponds to the point where the peaks of the slip curves are observed. Hence, the controller achieves the maximum utilisation of the adhesion in all cases. The test results are available in Figure 51 of the thesis.

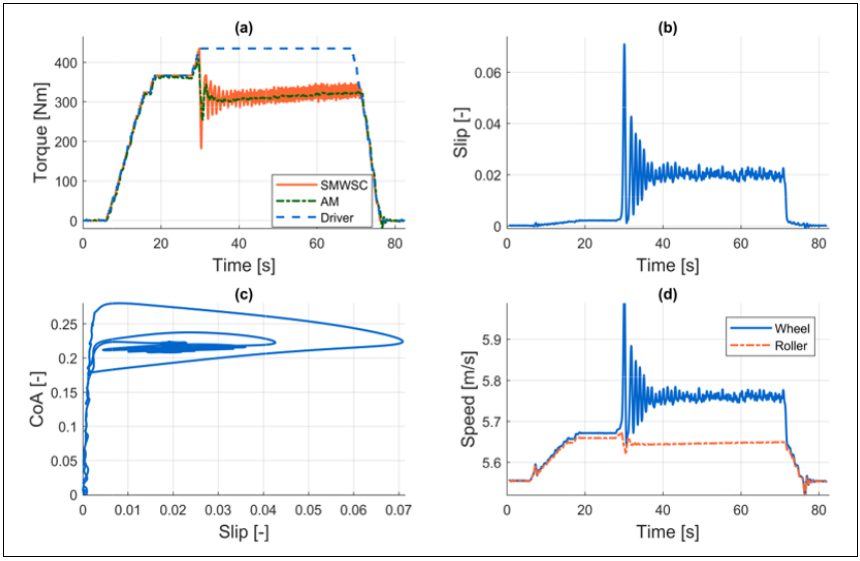

Figure 22. Experimental results of SM-WSC performed under water contaminated test condition.

5.4 Analysis of Results

The performances of the control methods are evaluated via experiments on a roller rig and simulations on its numerical model. The conditions of the simulations and experiments are employed identically to provide a comparative discussion.

When the simulation and experimental results for each method under the same test conditions are compared, it is obvious that both results are in good agreement.

Moreover, it is observed that the WSCST and WSCMT suppress the wheel slip slightly better than the WSCAA. On the other hand, the experimental tests summarised in Table 7 of the thesis show that WSCAA improves traction performance better than the WSCST and WSCMT. Consequently, the WSCAA strategy is primarily recommended to be used on EMUs due to its advantages (see section 4.3 of the thesis) over the other methods.

The performance evaluation of control strategies with different roller speeds, threshold values, deceleration rates and increment rates are conducted through the validated numerical model. Findings from the validated numerical model for the re-adhesion methods can be summarised as depicted in Table 1:

Table 1: Effect of increasing the control parameter on wheel slip

	WSCST	**WSCMT**	**WSCAA**
s_{th} / α_{th}	Increase	Increase	Increase
v_r	Decrease	Decrease	Decrease
A_{dec}	Increase	Increase	Increase
A_{inc}	Decrease	Decrease	Decrease

The assignment of threshold values (s_{th} and α_t) is very critical for the control process. When it is set higher, severe wheel slip is observed while lower values caused insufficient adhesion utilisation. Furthermore, A_{dec} is a vital control parameter which directly affects the convergence rate of the actual wheel slip. Selecting a high value for A_{dec} results in an excessive drop in the motor torque. If A_{dec} is set to a low entity, the wheel slip reaches very high levels. The control parameter A_{inc} determines the torque increase rate of the controller. Adjustment a small value for A_{inc} causes a slow torque recovery; nevertheless, selecting a higher value results in unstable wheel slip control.

The impact of each parameter on the control behaviour the PI-WSC and SM-WSC are summarised as follows:

PI-WSC method:

- The controller exhibits good wheel slip tracking performance with all roller speeds and all contact conditions. However, low amplitude vibrations are noticed at lower roller speeds.
- The controller provides successful performance under the water and grease contaminated test conditions when the desired wheel slip is set on the stable part of the slip curve. On the other hand, adjustment of the desired wheel slip to the unstable part of the slip curve brings the risk of control quality deterioration.
- Higher overshoot is observed with the lower proportional gain parameter (K_p) independent from the contact conditions. Moreover, the controller is capable of stabilising the wheel slip under grease contaminated case for lower K_p
- The integral gain parameter (K_i) influences the rise time to the desired set point. When K_i sets to a lower value, the higher rise time is observed.

SM-WSC method:

- The wheel slip overshoot increases slightly at higher roller speeds; however, the amplitude of vibrations reduces.
- The controller is able to stabilise wheel slip even on the unstable part of the slip curve.

- The convergence rate parameter (*D*) influences the damping of the wheel slip. The higher value of the convergence rate parameter causes higher overshoot and longer settling time.
- The uncertainties parameter (*K*) has no significant influence on the results.

The presented results show that both controllers are able to stabilise the wheel slip effectively when the desired wheel slip is set on the stable part of the slip curve. However, the performance of the PI-WSC deteriorates when the desired wheel slip is set on the unstable part of the slip curve. On the other hand, SM-WSC is able to stabilise wheel slip even on the unstable part. Hence, the application of the SM-WSC on electric locomotives is advised.

6 CONCLUSION

The work presented in the thesis is aimed to determine effective and viable solutions to wheel slip problem. Hence, Five wheel slip control strategies -wheel slip control based on single threshold (WSCST), wheel slip control based on multiple thresholds (WSCMT), wheel slip control based on angular acceleration of wheel (WSCAA), PI wheel slip control (PI-WSC), and sliding mode wheel slip control (SM-WSC)- are suggested. Initially, the validity of the developed numerical model is proven through the comparison of the numerical and experimental results. Then, the performances of the control methods are evaluated through experiments on a roller rig and simulation tests on the validated numerical model. Moreover, the influence of different roller speeds and control parameters are investigated through the validated numerical model since it provides an advantage by allowing us to set the identical test condition for each case.

It is observed that wheel slip control strategies based on the threshold value (WSCST, WSCMT and WSCAA) suppress the severe wheel slip effectively. Due to its advantages over the other methods, the WSCAA strategy is primarily recommended to be used on EMUs. The PI-WSC and SM-WSC successfully stabilise the wheel slip at a defined reference slip value. Furthermore, the PI-WSC and SM-WSC algorithms do not only stabilise the wheel slip but also help to establish optimum utilisation of the adhesion characteristic regardless of the severity of contaminants between the wheel and the roller when the optimal reference wheel slip is introduced. The SM-WSC has an advantage over the PI-WSC due to its useful properties in the stabilisation of nonlinear and uncertain systems. Hence, it is appropriate to use the SM-WSC on electric locomotives.

6.1 Completed Objectives of Doctoral Thesis

The completed objectives of the thesis are as follows:

(i) **Summarising a large number of published studies on the wheel slip, adhesion and slip control methods:** the gathered information about the adhesion, slip mechanism, wheel slip detection methods and wheel slip control methods are included in section 2, to give the reader a general overview of the research covered in the thesis.

(ii) **Reproducing a numerical model of the tram wheel roller rig in MATLAB environment that can be used for performance evaluation of the wheel slip control strategies:** In section 3.2, the numerical model of tram wheel roller rig, that is introduced in section 3.1, is reproduced in MATLAB environment.

(iii) **Proposing algorithms to control the wheel slip mechanism and establishing optimum utilisation of adhesion**: In section 4, the developed wheel slip control strategies are introduced. Strategies in sections 4.1, 4.2 and 4.3 are designed to be used on EMU while the strategies in sections 4.4 and 4.5 are designed to be used on electric locomotives.

(iv) **Validation of reproduced numeric model:** In section 5.1, the validity of the developed numerical model (see section 3.2) is proven by comparing simulation results with experimental results.

(v) **Verifying the functionality of proposed wheel slip control algorithms by either the validated numerical model or experimentally obtained results from the tram wheel roller rig:** In section 5.2, the functionality of the proposed wheel slip control algorithms is verified by the validated numerical model (under the assumption of several surface conditions). In section 5.3, the functionality of the controllers is proven with the experimental setup under several test conditions.

(vi) **Performance evaluation of the proposed wheel slip control algorithms with different speeds and control parameters:** The validated numerical model is used for the further performance evaluation of the wheel slip control algorithms with different speeds and control parameters. The simulation results are presented in the Appendices of the thesis. The summaries of the simulations are presented in section 5.4.

6.2 Scientific Contributions of Doctoral Thesis

An advanced numerical model of a tram wheel roller rig that includes nonlinear effects caused by time delay and disturbances to match the values of the experimental test setup is developed so that other researchers can easily

simulate the dynamic responses of wheel slip and electric motor control strategies.

Three different re-adhesion (WSCST, WSCMT and WSCAA) are suggested for the use on the EMUs. The WSCST and WSCAA are conventional re-adhesion strategies. Employing WSCMT on wheel slip control is unique and proposed by the author. It aims to provide an improvement to the utilisation of the adhesion.

Two more different strategies (PI-WSC and SM-WSC) for the use of electric locomotive are also proposed in this thesis. It is known that the PI-WSC method is widely used for industrial applications. However, the wheel slip control stability cannot be guaranteed with the PI controllers due to their linear characteristics [11]. On the other hand, SM-WSC is an attractive robust control method which has effective properties to stabilise the nonlinear and uncertain systems. The author has modified and applied a control strategy which is presented for a personal electric vehicle in the previous literature [33]. According to the author's knowledge, SM-WSC is an original control strategy in the related literature which aims to stabilise the wheel slip for a roller rig.

The dynamic responses of the implemented anti-slip control strategies are evaluated under different surface conditions (half-dry, wet, greasy and wet&greasy) on both experimental tram wheel roller rig and its numeric model. Furthermore, the performance of the control strategies with different speeds, threshold values, deceleration and increment rates are evaluated on the validated numerical model. The carried-out simulations and experiments bring considerable knowledge in the scientific field.

6.3 Future Works

The purpose of the slip control methods is to prevent the wheel from severe slip and improve the traction effort of the vehicle. Furthermore, the development of such systems is very critical for the safety of the vehicles. Hence, we have presented five of the wheel slip control strategies. Tests carried out on the experimental roller rig and its numerical model verify the presented strategies. The further verification of the developed strategies can be carried on the real locomotive in future. Another future work can be the development of optimal reference slip ratio seeking algorithm. In this work, the reference value of the wheel slip is obtained from the experimental measurements (predefined reference value). However, it is possible to obtain the reference using the characteristic slip curve. Hence, it is planned to adopt the recursive least square with the steepest gradient method (RLS-SGM) to determine the optimal wheel slip ratio online for the presented control strategies.

REFERENCES

[1] P. Pichlík, “Strategy of Railway Traction Vehicles Wheel Slip Control,” CZECH TECHNICAL UNIVERSITY, Prague, 2018.

[2] H. Chen, T. Ban, M. Ishida, and T. Nakahara, “Experimental investigation of influential factors on adhesion between wheel and rail under wet conditions,” *Wear*, vol. 265, no. 9–10, pp. 1504–1511, Oct. 2008.

[3] C. W. Jenks, “Improved Methods for Increasing Wheel/Rail Adhesion in the Presence of Natural Contaminants,” Transit Co-operative Research Program, Research Results Diges, 17, 1997.

[4] J. Yu, “Re-adhesion control for railway traction systems,” The University of Leeds, Leeds, 2007.

[5] W. J. Wang, H. F. Zhang, H. Y. Wang, Q. Y. Liu, and M. H. Zhu, “Study on the adhesion behavior of wheel/rail under oil, water and sanding conditions,” *Wear*, vol. 271, no. 9–10, pp. 2693–2698, Jul. 2011.

[6] H. Chen, T. Ban, M. Ishida, and T. Nakahara, “Adhesion between rail/wheel under water lubricated contact,” *Wear*, vol. 253, no. 1–2, pp. 75–81, Jul. 2002.

[7] E. A. Gallardo-Hernandez and R. Lewis, “Twin disc assessment of wheel/rail adhesion,” *Wear*, vol. 265, no. 9–10, pp. 1309–1316, Oct. 2008.

[8] R. Lewis, R. S. Dwyer-Joyce, S. R. Lewis, C. Hardwick, and E. A. Gallardo-Hernandez, “Tribology of the Wheel-Rail Contact: The Effect of Third Body Materials,” *Int. J. Railw. Technol.*, vol. 1, no. 1, pp. 167–194, Apr. 2012.

[9] Z. Li, O. Arias-Cuevas, R. Lewis, and E. A. Gallardo-Hernández, “Rolling–Sliding Laboratory Tests of Friction Modifiers in Leaf Contaminated Wheel–Rail Contacts,” *Tribol. Lett.*, vol. 33, no. 2, pp. 97–109, Feb. 2009.

[10] M. Malvezzi, L. Pugi, S. Papini, A. Rindi, and P. Toni, “Identification of a wheel–rail adhesion coefficient from experimental data during braking tests,” *Proc. Inst. Mech. Eng. Part F J. Rail Rapid Transit*, vol. 227, no. 2, pp. 128–139, Mar. 2013.

[11] D. Frylmark and S. Johnsson, “Automatic Slip Control for Railway Vehicles,” Linköpings Universitet, Linköpings, 2003.

[12] Z. Zhu, K. Yuan, W. Zou, and H. Hu, “Current-based wheel slip detection of all-wheel driving vehicle,” in *2009 International Conference on Information and Automation*, Zhuhai, Macau, China, 2009, pp. 495–499.

[13] P. Pichlík, “Overview of Slip Control Methods Used in Locomotives,” *Trans. Electr. Eng.*, vol. 3, no. 2, pp. 38–43, 2014.

[14] J. Huang, J. Xiao, D. Zhao, and S. Wang, “A wheel slip detection method of electric locomotive based on time-frequency analysis,” in *International Conference on Intelligent Transportation Systems*, Qingdao, China, 2014, pp. 1221–1225.

[15] M. Amiri and B. Moaveni, “Vehicle velocity estimation based on data fusion by Kalman filtering for ABS,” in *20th Iranian Conference on Electrical Engineering (ICEE2012)*, Tehran, Iran, 2012, pp. 1495–1500.
[16] B. Moaveni, M. Khosravi Roqaye Abad, and S. Nasiri, “Vehicle longitudinal velocity estimation during the braking process using unknown input Kalman filter,” *Veh. Syst. Dyn.*, vol. 53, no. 10, pp. 1373–1392, Oct. 2015.
[17] L. Imsland, T. A. Johansen, T. I. Fossen, H. Fjær Grip, J. C. Kalkkuhl, and A. Suissa, “Vehicle velocity estimation using nonlinear observers,” *Automatica*, vol. 42, no. 12, pp. 2091–2103, Dec. 2006.
[18] L. Imsland, T. A. Johansen, T. I. Fossen, J. C. Kalkkuhl, and A. Suissa, “Vehicle Velocity Estimation using Modular Nonlinear Observers,” in *Proceedings of the 44th IEEE Conference on Decision and Control*, Seville, Spain, 2005, pp. 6728–6733.
[19] D. M. Bevly, J. C. Gerdes, and C. Wilson, “The Use of GPS Based Velocity Measurements for Measurement of Sideslip and Wheel Slip,” *Veh. Syst. Dyn.*, vol. 38, no. 2, pp. 127–147, Feb. 2003.
[20] M. Joos, J. Ziegler, and C. Stiller, “Low-cost sensors for image based measurement of 2D velocity and yaw rate,” in *IEEE Intelligent Vehicles Symposium*, San Diego, CA, USA, 2010, pp. 658–662.
[21] K. Kondo, “Anti-slip control technologies for the railway vehicle traction,” in *2012 IEEE Vehicle Power and Propulsion Conference*, Seoul, South Korea, 2012, pp. 1306–1311.
[22] P. Voltr and M. Lata, “Transient wheel–rail adhesion characteristics under the cleaning effect of sliding,” *Veh. Syst. Dyn.*, vol. 53, no. 5, pp. 605–618, May 2015.
[23] P. Voltr, “Simulation of wheel-rail contact conditions on experimental equipment,” *Railw. Transp. Logist.*, vol. 11, pp. 77–82, 2015.
[24] J. Gerlici, M. Gorbunov, K. Kravchenko, O. Nozhenko, and T. Lack, “Experimental rigs for wheel/rail contact research,” *Manuf. Technol.*, vol. 16, no. 5, pp. 909–916, 2016.
[25] P. Voltr, M. Lata, and O. Cerny, “Measuring of wheel-rail adhesion characteristics at a test stand,” in *18th International Conference Engineering Mechanics*, Svratka, Czech Republic, 2012, pp. 1543–1553.
[26] A. Onat, P. Voltr, and M. Lata, “An unscented Kalman filter-based rolling radius estimation methodology for railway vehicles with traction,” *Proc. Inst. Mech. Eng. Part F J. Rail Rapid Transit*, vol. 232, no. 6, pp. 1686–1702, 2017.
[27] A. Onat, A. Zirek, and P. Voltr, “Dynamic Modelling and Numerical Simulation of a Tram Wheel Test Stand,” in *3rd International Symposium on Electrical Railway Transportation Systems, ERUSIS 2017, Eskisehir, Turkey*, 2017.

[28] A. Apte, R. Walambe, V. Joshi, K. Rathod, and J. Kolhe, “Simulation of a permanent magnet synchronous motor using matlab-simulink,” in *2014 Annual IEEE India Conference (INDICON)*, Pune, India, 2014, pp. 1–5.
[29] J. Simanek, J. Novak, O. Cerny, and R. Dolecek, “FOC and flux weakening for traction drive with permanent magnet synchronous motor,” in *2008 IEEE International Symposium on Industrial Electronics*, Cambridge, UK, 2008, pp. 753–758.
[30] A. W. Leedy, “Simulink/MATLAB dynamic induction motor model for use as a teaching and research tool,” *Int. J. Soft Comput. Eng.*, vol. 3, no. 4, pp. 102–107, 2013.
[31] J. Simanek, J. Novak, R. Dolecek, and O. Cerny, “Control Algorithms for Permanent Magnet Synchronous Traction Motor,” in *The International Conference on “Computer as a Tool,”* Warsaw, Poland, 2007, pp. 1839–1844.
[32] O. Polach, “Creep forces in simulations of traction vehicles running on adhesion limit,” *Wear*, vol. 258, no. 7–8, pp. 992–1000, Mar. 2005.
[33] K. Nam, Y. Hori, and C. Lee, “Wheel Slip Control for Improving Traction-Ability and Energy Efficiency of a Personal Electric Vehicle,” *Energies*, vol. 8, no. 7, pp. 6820–6840, Jul. 2015.
[34] D. Caporale, P. Colaneri, and A. Astolfi, “Adaptive nonlinear control of braking in railway vehicles,” in *52nd IEEE Conference on Decision and Control*, Florence, Italy, 2013, pp. 6892–6897.
[35] L. Jin and Y. Liu, “Study on Adaptive Slid Mode Controller for Improving Handling Stability of Motorized Electric Vehicles,” *Math. Probl. Eng.*, vol. 2014, pp. 1–10, 2014.
[36] J. J. E. Slotine and W. Li, *Applied Nonlinear Control*. NJ, USA,: Prentice-Hall: Englewood Cliffs, 1991.
[37] J. S. Kim, S. H. Park, J. J. Choi, and H. Yamazaki, “Adaptive Sliding Mode Control of Adhesion Force in Railway Rolling Stocks,” in *Sliding Mode Control*, Rijeka, Croatia: InTech, 2011, pp. 385–408.
[38] W. Gao and J. C. Hung, “Variable structure control of nonlinear systems: A new approach,” *IEEE Trans. Ind. Electron.*, vol. 40, no. 1, pp. 45–55, 1993.
[39] K. Nam, H. Fujimoto, and Y. Hori, “Design of an adaptive sliding mode controller for robust yaw stabilisation of in–wheel–motor–driven electric vehicles,” *Int. J. Veh. Des.*, vol. 67, no. 1, pp. 98–113, 2014.

PUBLICATIONS OF STUDENT

A. Zirek, P. Voltr, M. Lata, and J. Novák, "An adaptive sliding mode control to stabilize wheel slip and improve traction performance," *Proceedings of the Institution of Mechanical Engineers, Part F: Journal of Rail and Rapid Transit*, vol. 232, no. 10, pp. 2392–2405, May 2018.

A. Onat, **A. Zirek**, and P. Voltr, "Dynamic Modelling and Numerical Simulation of a Tram Wheel Test Stand," in *3rd International Symposium on Electrical Railway Transportation Systems, ERUSIS 2017,* Eskisehir, Turkey, 2017.

P. Voltr, **A. Zirek**, and B. T. Kayaalp, "New Experience and Results from Experimental Measurement of Adhesion on a Roller Rig," in *23rd International Conference on Current Problems in Rail Vehicles,* Ceska Trebova, Czech Republic, 2017, pp. 423-432

A. Zirek and B. T. Kayaalp, "The Slip Control of a Tram-Wheel Test Stand Model with Single Neuron PID Control Method," in *VII. International Scientific Conference of the Faculty of Transport Engineering*, Pardubice, Czech Republic, 2018, pp. 268-275